Phys. Biol. **4** (2007) R1–R17 doi:10.1088/1478-3975/4/2/R01

REVIEW ARTICLE

Oscillations and temporal signalling in cells

G Tiana[1], S Krishna[2], S Pigolotti[3], M H Jensen[2] and K Sneppen[2]

[1] Department of Physics, University of Milano and INFN via Celoria 16, 20133 Milano, Italy
[2] The Niels Bohr Institute, Bledgamsvej 16, 2100 Copenhagen, Denmark
[3] Instituto de Fisica Interdisciplinar y Sistemas Complejos IFISC (CSIC-UIB), Campus de la Universitat de les Illes Balears, E-07122 Palma de Mallorca, Spain

Received 9 March 2007
Accepted for publication 2 May 2007
Published 18 May 2007
Online at stacks.iop.org/PhysBio/4/R1

Abstract
The development of new techniques to quantitatively measure gene expression in cells has shed light on a number of systems that display oscillations in protein concentration. Here we review the different mechanisms which can produce oscillations in gene expression or protein concentration using a framework of simple mathematical models. We focus on three eukaryotic genetic regulatory networks which show 'ultradian' oscillations, with a time period of the order of hours, and involve, respectively, proteins important for development (Hes1), apoptosis (p53) and immune response (NF-κB). We argue that underlying all three is a common design consisting of a negative feedback loop with time delay which is responsible for the oscillatory behaviour.

1. Introduction

Biological systems display fascinating spatial and temporal patterns, which hint that the underlying cellular processes are highly dynamic and operate on a wide range of time- and lengthscales. This is indeed confirmed by measurements of the temporal dynamics of protein concentrations and gene expression levels for various signalling and response systems, made using pulse-labelling [1], β-galactosidase measurements and immunoblotting [2], electromobility shift assays [3], real time PCR [4], fluorescence techniques [5–8], chromatin immunoprecipitation assays [9] and microarrays [10]. Overall, it is now evident that regulatory and signal transduction networks do not depend merely on shifting the relevant protein concentrations from one steady state level to another. Rather, the signals often have a significant temporal variation that carries much more information and propagates through the regulatory networks in a complex manner. With time-resolved data now available for a number of response and signalling systems, it is perhaps the appropriate time to explore whether there are any commonalities, or 'design principles', in the underlying mechanisms. In this review we will show that a prominent subclass of such systems does indeed have a common underlying design structure which combines a negative feedback loop with a time delay.

This subclass consists of systems that display oscillatory behaviour under some conditions. The most obvious examples are circadian rhythms and cell division. Oscillations are also seen in the levels of cellular calcium [11] and in embryo development. Somite segmentation, for instance, exhibits clearly periodic spatial patterns which are produced by periodic temporal variation of proteins such as Hes1, Axin, Notch and Wnt [12–15]. We also include in this class systems which display damped oscillations or semi-periodic behaviour. One example is oscillations, triggered by DNA damage, in p53, a key protein involved in cell death and apoptosis pathways [5, 6, 16, 17]. Hormones, such as the human growth factor, also show such intermittently periodic behaviour and pulsatile secretion [18]. For these systems the recurrent behaviour probably has a direct physiological role. In cyanobacteria, for example, various physiological processes, such as respiration and carbohydrate synthesis, are directly influenced by the circadian clock to be in sync with the day–night cycle [19]. For other systems, however, clear oscillatory behaviour is not observed in the wild-type, but only in certain mutants. For instance, the NF-κB signalling system, involved

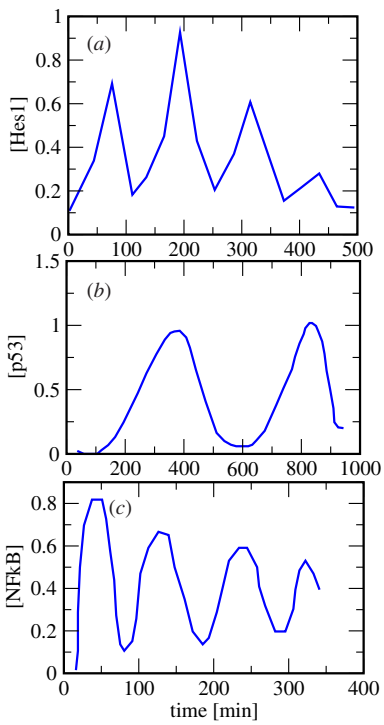

Figure 1. Experimentally observed 'ultradian' oscillations in (*a*) Hes1, data taken from [12], (*b*) p53, data taken from [5] and (*c*) NF-κB, data taken from [3]. The concentrations are in arbitrary units.

in immune response in mammalian cells, shows oscillations in nuclear NF-κB concentration only in a mutant which contains just one isoform of the NF-κB inhibitor, IκBα, and not the other isoforms [3]. Fluorescence measurements of the NF-κB system modified so that IκBα was overexpressed also showed sustained oscillations over several hours [7]. However, wild-type cells show at best damped oscillations [3]. Here it is not clear if the oscillations themselves have a significant physiological consequence or are merely a by-product of other requirements for the wild-type behaviour. Nevertheless, the sub-parts of these systems which are potentially oscillatory are important, often essential, components which influence the complex temporally varying wild-type response.

We will focus on three of the regulatory systems mentioned above: Hes1 in mammalian embryos, p53-Mdm2 in mammalian cells, and the NF-κB signalling system, also in mammalian cells. Figure 1 shows the oscillations observed in experiments for all three. These systems are quite complicated, with many components interacting in various ways, including transcriptional activation/repression, translation and post-translation regulation, protein–protein interaction, targeted protein degradation and active nuclear–cytoplasmic translocation, composed into a complex network with multiple feedback loops. In this review, we mainly describe the mechanisms and structures in these networks that allow them to produce the observed oscillations. We will do this using simplified mathematical models where the level of description balances the need to correctly describe the systems with the need to coarse-grain over some details in order to reveal common design features.

We first begin by defining the overall framework of models we consider, and describing the basic ingredients for producing oscillatory behaviour within this framework. In the subsequent sections we show how the three examples of Hes, p53 and NF-κB contain these ingredients. Therein we also elaborate, using stability analysis, the requirements for producing oscillations in these systems. Finally, we briefly discuss how to extract information about underlying structures from oscillatory time series data.

Our analysis does indeed reveal that these three systems have a common underlying design, consisting of a *negative feedback loop* with an effective *time delay*. Among the many ways of producing a time delay, we emphasize the mechanism of *saturated degradation*, where the degradation rate of a protein saturates at high concentrations of that protein. This can happen when the protein is actively degraded by another enzyme, and the degradation rate is limited by that enzyme rather than the protein concentration. The importance and generality of saturated degradation are discussed further in the final section. There we also speculate on the physiological function of oscillations. While it is unclear whether the oscillations in themselves have a direct physiological importance, we suggest that they can carry much more information than steady state signals. For instance, oscillations can be very spiky and in the NF-κB system we show that such spiky oscillations can be used to produce very sharp response with large effective Hill coefficients. Thus we argue that oscillations, in particular spiky ones, have interesting properties that could be exploited by gene regulatory systems.

1.1. Negative feedback

Figure 2(*a*) shows a schematic negative feedback loop. The individual nodes in this loop are the relevant dynamical variables: they could be protein concentrations, gene expression levels, etc. Each variable either activates or represses the next one in the loop. By an activator, we mean that if the concentration of protein 1 goes up it tends to increase the concentration of protein 2 (either by increasing its production rate or decreasing its degradation rate). A repressor has the opposite effect. Then, a negative feedback loop is simply defined as *a loop with an odd number of repressors*, so that the effect of a perturbation in the concentration of any species in the loop eventually feeds back to itself with a negative sign. Feedback loops are, in general, the most common network motifs in cellular organization, especially when one considers the regulation of small molecules [20]. We concentrate on negative feedback here because it was hypothesized by Thomas [21], and rigorously proven for a wide class of systems [22, 23] that the presence of at least one negative feedback loop is a necessary condition for oscillations.

The simplest negative feedback loop is of course a protein which represses itself. There are many examples of such proteins: the main repressor of the SOS regulon in *E. coli*, LexA, also represses its own production [24]; Hes1, mentioned above, also represses transcription of its own gene [12], shown

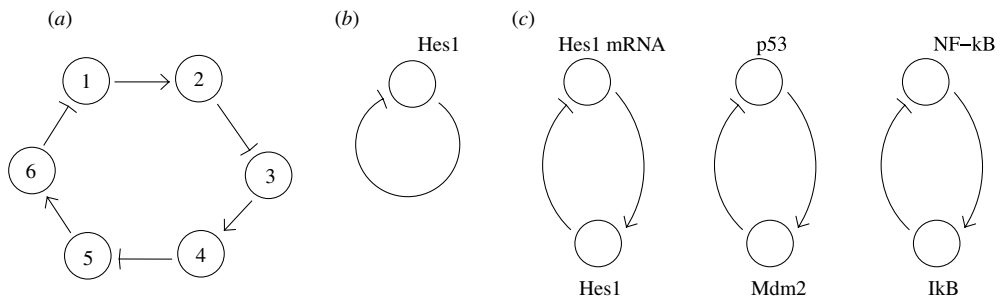

Figure 2. Negative feedback loops: (*a*) a generic multi-species negative feedback loop; (*b*) the simplest negative feedback loop—a self-repressor; (*c*) two-component negative feedback loops for the three examples we examine. In all figures a normal arrow represents an activating interaction, and a barred arrow represents a repressing interaction.

schematically in figure 2(*b*). However, Hes1 looks like a one-component loop only if we coarse-grain over the intermediate steps in protein production. If we also count the Hes1 mRNA then it becomes the two-component negative feedback loop of figure 2(*c*): one component, Hes protein, represses the production of the second, Hes1 mRNA, while the second component activates the first. The other two systems we discuss later in this review have the same loop structure when coarse-grained to the two-component level. Nuclear NF-κB is known to activate production of IκBα, which inhibits nuclear import of NF-κB by sequestering it in the cytoplasm [3]. p53 and Mdm2 work similarly, with p53 activating the *mdm2* gene and Mdm2 sequestering p53 [25].

To examine the possible dynamical behaviour produced by a negative feedback loop, we model the dynamics of the concentrations of the components using ordinary coupled differential equations. For instance, for the two-component loops shown in figure 2(*c*),

$$\frac{\mathrm{d}x_1}{\mathrm{d}t} = g_1(x_1, x_2) \qquad \frac{\mathrm{d}x_2}{\mathrm{d}t} = g_2(x_1, x_2), \tag{1}$$

where x_1 and x_2 are the concentrations of the two components X_1 and X_2. This can easily be generalized to longer loops with N components,

$$\frac{\mathrm{d}x_i}{\mathrm{d}t} = g_i(x_i, x_{i-1}), \qquad i = 1, 2, \ldots, N, \tag{2}$$

which models a single feedback loop with no cross-links because the rate of change of a given variable x_i depends only on itself and the preceding variable, x_{i-1}. In writing such an equation we are assuming that fluctuations in space and time are negligible. Thus, there are no stochastic or diffusion terms. The functions g_i model both production and degradation of the components, and can take many forms depending on the kind of interactions in the system. For example, in the p53 example (with $X_1 \to$ p53, $X_2 \to$ Mdm2), we know that p53 binds to an operator site at the promoter for the *mdm2* gene and aids transcription. Then, under some assumptions[4] the production of Mdm2 can be modelled using a term of the form

$$\frac{(p/K)^h}{1 + (p/K)^h}, \tag{3}$$

a sigmoidal monotonically increasing function of the p53 concentration, p (the Hill coefficient, $h \geqslant 1$, accounts for cooperativity in the binding of p53 to the operator, and K is the dissociation constant).

It is difficult to say anything about the behaviour of the general coupled differential equation of a negative feedback loop, such as equation (2). However, it is reasonable to constrain the functions g_i of equation (2) to be monotonic in x_{i-1}. This corresponds to saying that a protein that activates a particular process cannot change to repress it at some other concentration, and vice versa, which is the case for most transcription factors[5]. For monotone systems, not only is there no ambiguity about whether the loop implements negative or positive feedback, but we can also prove rigorously that there is only one fixed point (see appendix A). The question then is whether such a steady state is stable or unstable. If the fixed point is unstable, and the system's trajectories are bounded (again, a reasonable assumption for a biological system) then it must show periodic oscillations: this is known as the Poincaré–Bendixson theorem [28]. On the other hand, in the case of two-variable monotonic systems, it is possible to show by Dulac's criterion [29] that oscillations are not possible (see appendix C).

1.2. Time delays

Physically, what is required for instability of the fixed point, and hence oscillations, is a time delay, or a slowing down of the signal going round the loop. By signal we mean perturbations of the concentrations away from the steady state. If a perturbation in the concentration of one variable instantaneously affects the concentration of the next one, and so on, then for a negative feedback loop any perturbation will be immediately cancelled and the steady state will be stable. A sufficiently large time delay on the other hand will produce oscillations. This can be readily understood with an example: consider a person who walks along a straight line to a given

[4] In particular, this assumes that the number of proteins bound to the operator site is much smaller than the total number of proteins.

[5] Some proteins can both activate as well as repress the same process depending on their concentration. For instance, CI in lambda phage activates the P_{RM} promoter at low concentrations, but represses it at high concentrations [26]. Another example is the galactose regulator GalR, which at high concentrations of galactose activates the promoter *galP2* but in the absence of galactose forms a DNA loop, which completely represses *galP2* [27]. Such examples are, however, somewhat rare and we will not consider them.

Table 1. Timescales of some processes in eukaryotic cells associated with a single molecule. The upper part of the table indicate the processes which are usually neglected in writing the rate equations of regulation networks, while the lower part indicate processes which are usually accounted for.

Translocation through nuclear pores [39]	10^{-4} s
Molecular diffusion in the cell	1 s
Translation [40]	30 s
Transcription [40]	3 min
mRNA degradation [40]	3 min
Protein degradation	10 min to 10 h
Cellular signals [3, 12, 16]	1 h

point, marked on the ground. If this person is able to take instantaneous decisions, he will approach the mark and then stop. This is a stationary solution to the walk kinetics. If, on the other hand, it takes some time to realize that the mark has been reached, the person will not stop at the mark, but cross it. When eventually the information that the mark has been crossed is processed, the person will turn back and walk in the opposite direction. The mark will again be reached and overshot, and so on. The resulting kinetics will be damped or sustained oscillations about the mark. In cellular systems many processes could produce time delays. Table 1 lists some timescales associated with such processes.

With the above insight, one can see that a simple way to model oscillations using the framework of equation (1) is to introduce an explicit time delay into the equations

$$\begin{aligned} \frac{\mathrm{d}x_1(t)}{\mathrm{d}t} &= g_1(x_1(t), x_2(t), x_1(t-\tau_1), x_2(t-\tau_2)) \\ \frac{\mathrm{d}x_2(t)}{\mathrm{d}t} &= g_2(x_1(t), x_2(t), x_1(t-\tau_3), x_2(t-\tau_4)). \end{aligned} \tag{4}$$

Of course, this is the most general form, and often it is possible to have fewer than four delays. Oscillations are observed even in the simplest case of a linear differential equation with a single (sufficiently large) delay (see appendix C), $\mathrm{d}x/\mathrm{d}t = -x(t-\tau)$, which models the one-component Hes loop of figure 2(*b*) where Hes1 represses itself after a time delay τ. Although a linear delay rate equation is an oversimplification of Hes1 production, the physics which lies behind more general delay differential equations such as equation (4) is the same. The added complication is that the functions g_1 and g_2 are in general highly nonlinear, resulting in an amplification of the effect of the delay.

Putting an explicit time delay like this, of course, does not really shed light on the mechanism producing the time delay. There are several possibilities which can be used to produce oscillations in a negative feedback loop:

(i) a process that takes a finite minimum time,
(ii) many intermediate steps,
(iii) a sharp response by some of the variables,
(iv) saturated degradation and
(v) autocatalysis.

To elaborate:

(i) Rate equations, such as equation (2), typically model processes which occur with a given average rate, such as the binding of a protein to an operator site. A hidden assumption is that the time interval between two binding events is Poisson distributed, which means that often there is a reasonable probability for two events to be separated by a very short time interval (say, much shorter than the average time between events). Sometimes, however, molecular processes take a certain minimum time. For instance, if transcription and translation take a time τ after a polymerase binds to the promoter, then the rate of production of the protein is more appropriately modelled as $\mathrm{d}x/\mathrm{d}t \propto P(t-\tau)$, where $P(t)$ is 1 if the polymerase is bound to the promoter at time t, and zero otherwise. Such logic has been used to justify time-delay models in a variety of systems [30, 32, 33]. This is the approach we will take to model the p53 and Hes systems, discussed in the subsequent sections.

(ii) Processes such as transcription and translation have this character because they are in fact composed of a large number of intermediate processes: the polymerase binds, first forming a closed complex, which then makes a transition to an open complex, and then to an elongating complex, followed by many 'steps' along the DNA until the polymerase reaches the end of the gene. Even if each of these individual steps is a Poisson process, the net effect adds up to a time delay. Thus, instead of putting in an explicit time delay as in equation (4), one could work with a negative feedback loop with many components. One simple example of such an oscillator is the repressilator [34], which is a negative feedback loop with six components.

(iii) The repressilator also has another necessary ingredient—a nonlinearity in the g_i functions which allows some of the variables to respond to changes in the preceding variable in a faster-than-linear fashion. More precisely, the repressilator uses sigmoidal functions, such as function (3), to describe transcriptional repression, and needs Hill coefficients of at least 2 in order to achieve oscillations. The earliest example of a negative feedback oscillator which uses a nonlinearity like this to produce a sharp response is a model by Goodwin [35], where the Hill coefficient needs to be more than 8.

(iv) Such high Hill coefficients are unlikely for biological systems, however. In order to get around this 'problem', Bliss, Painter and Marr [36] introduced another way of producing an effective time delay. They used the saturated degradation of one of the concentrations. Saturated degradation means that there is an upper limit to the degradation rate of one species, thereby allowing it to remain abundant for a longer time, thus effectively slowing down the signal travelling around the loop. Such saturated degradation is quite common in biological systems, especially when proteins are tagged for targeted degradation by another protein, as we will show in the NF-κB case discussed below.

(v) Finally, autocatalysis, where a molecule activates its own production can be used to produce oscillations in systems such as equation (1) [37]. In fact for two variable systems where there is no explicit time delay this is a necessary

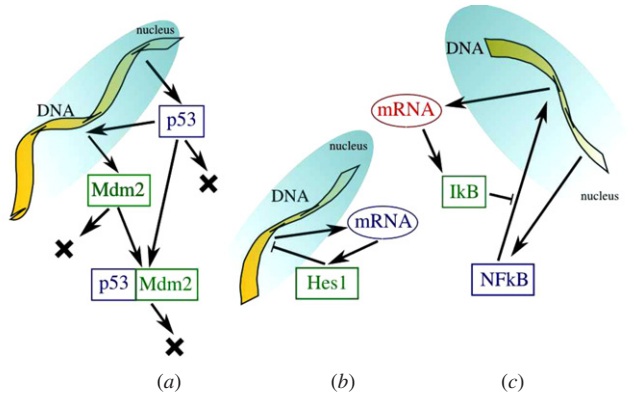

Figure 3. A sketch of the feedback loops controlling the concentration of p53 (*a*), Hes1 (*b*) and NF-κB (*c*).

condition for oscillations [38]. Note that this modification typically makes the system non-monotonic.

This survey of the theoretical requirements for producing oscillations in negative feedback loops already allows us to make an interesting observation: monotone two-component loops without an explicit time delay cannot oscillate, whatever the nonlinearity in the g_i functions. We prove this explicitly in appendix C. Thus, if one insists on modelling an oscillating system using two variables, one must choose between introducing a time delay, and sacrificing monotonicity.

2. Ultradian oscillations in biological systems

We now turn to three biological systems to illustrate these ideas in action. In the following, we will briefly give a description of the systems, p53-Mdm2, Hes1 and NF-κB, in which 'ultradian' oscillations have been observed, which have time periods of the order of hours, as opposed to 'circadian' 24 h rhythms. We will discuss specific details of each system, at the same time emphasizing that the basic physical mechanism which produces oscillations in all three is the same—negative feedback along with time delays.

2.1. p53-Mdm2

The protein p53 is responsible for inducing apoptosis in cells with damaged DNA [41]. The concentration of p53 is usually kept low by a feedback mechanism involving another protein, Mdm2, which binds to p53 and promotes its degradation. When the DNA is damaged, the cell expresses a number of kinases which phosphorylate SER20 in p53, changing its affinity to Mdm2. This results in oscillations in the concentration of p53, observed both in western blot analysis [16, 42] (cf figure 1(*a*)) and in single cell fluorescence experiments [5, 6]. The standard explanation for the overall increase in the concentration of p53 is that its phoshoprylation decreases its affinity to Mdm2, shifting the thermodynamic equilibrium towards higher concentrations.

Apart from not explaining the oscillations, this argument does not agree with other experimental evidence. Equilibrium isothermal titration calorimetry experiments have shown [43] that phosphorylation at SER20 *decreases*, not increases, the dissociation constant between p53 and Mdm2 from $k_D = 575 \pm 19$ nM to $k_D = 360 \pm 3$ nM. The same effect is observed *in vivo* [44], where p53ASP20 (a mutated form which mimics phosphorylated p53) binds Mdm2 more tightly than p53ALA20 (which mimics unphosphorylated p53). Moreover, single cell experiments [5] show a slight decrease in the concentration of p53 after DNA damage, which cannot be explained by the standard argument.

We showed that a simple model of the p53-Mdm2 system that incorporates the time delay associated with some relatively slow processes within the cell can account for the experimental facts in a simple way [30]. The feedback mechanism is sketched in figure 3(*a*) and the associated time-delayed rate equations are

$$\begin{aligned} \frac{\mathrm{d}p}{\mathrm{d}t} &= S - a \cdot r - b \cdot p \\ \frac{\mathrm{d}m}{\mathrm{d}t} &= c\frac{p(t-\tau) - r(t-\tau)}{k_g + p(t-\tau) - r(t-\tau)} - d \cdot m \\ r &= \frac{1}{2}\left((p+m+k) - \sqrt{(p+m+k)^2 - 4p \cdot m}\right), \end{aligned} \tag{5}$$

where p, m and r are the concentrations of p53, Mdm2 and of the complex p53-Mdm2, respectively. In the first equation, S is the expression rate of p53, a is the Mdm2-mediated degradation rate of p53 and b is the spontaneous degradation rate of p53. In the second equation, c is the p53-mediated expression rate of Mdm2 and d is the spontaneous degradation rate of Mdm2. The delay τ takes into account the half-life of mRNA, the diffusion time, the time needed to cross the nuclear membrane and the transcription/translation time. The last equation gives the concentration r of the p53–Mdm2 complex, under the equilibrium assumption. One can solve equations (5) numerically, simulating the damage to DNA by a sudden change in the dissociation constant k. Figure 4 shows the onset of oscillations in this model in response to a sudden decrease in k at time $t = 2000$ s.

Several observations emerge from the simulation results in figure 4. Most interestingly, what triggers oscillations is a decrease in the dissociation constant k, while any increase in its value just shifts the equilibrium towards higher values of p (cf the inset of figure 4). Moreover, just after $t = 2000$ s the concentration of p53 decreases, as observed in the experiments. Finally, the concentration, r, of the complex p53-Mdm2 is, at any time, essentially identical to the minimum of p and m (grey curve in figure 4), indicating that the complex is saturated, in the sense that essentially all possible complex is formed (i.e., $r \approx \min(p, m)$).

The relative change, Δp, in the maximum concentration of p53 reached after the simulated stress event is displayed in figure 5 as a function of the change in k. The value of Δp displays a sigmoidal behaviour if the stress decreases the value of k. In contrast, in the absence of a time delay, this curve is linear with respect to k [30]. Thus, the time delay and the oscillations are crucial for producing a sensitive system that can respond to stress in a sharp, faster-than-linear manner.

We also undertook a detailed analysis of the response of the oscillations to changes in the parameters [30]. It turns

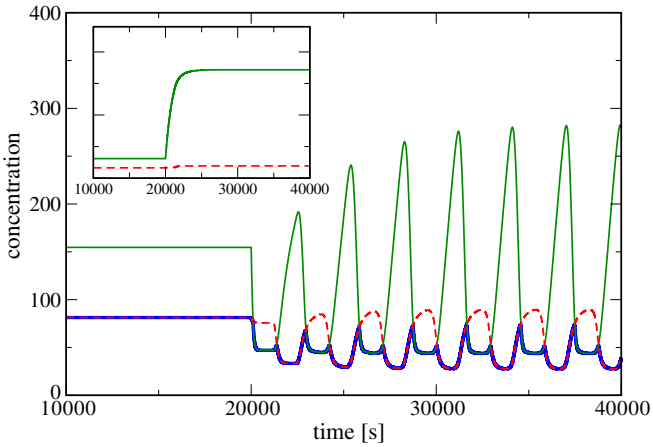

Figure 4. Oscillations displayed by the numerical solution of the dynamic equations of p53. The concentration of p53 is displayed with a green curve, that of Mdm2 with a red dashed curve and that of the p53–Mdm2 complex with a blue curve. The numerical values of the rates are $a = 3 \times 10^{-2}\ \mathrm{s}^{-1}$, $b = 10^{-4}\ \mathrm{s}^{-1}$, $c = 1\ \mathrm{s}^{-1}$, $d = 1\ \mathrm{s}^{-2}$, $S = 1\ \mathrm{s}^{-1}$, $k = 180$, $k_g = 28$ and $\tau = 1200$ s. At time $t = 20\,000$ s the value of k is decreased by a factor of 10. In the inset, the solution of the same equations, where the value of k is increased by a factor of 10 at $t = 20\,000$ s. The equations are solved with the Adams algorithm [31].

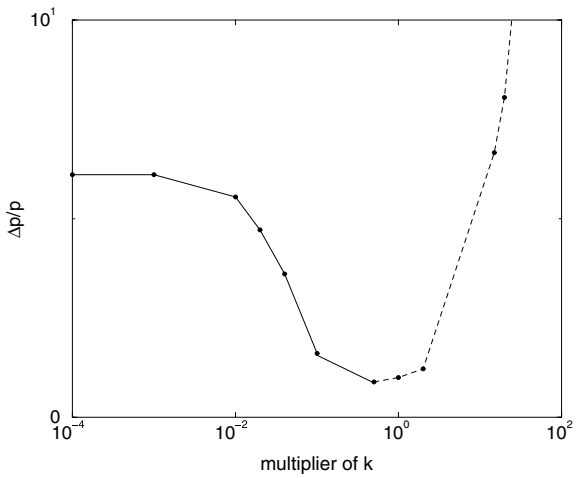

Figure 5. The height of the maximum response peak Δp with respect to the quantity that multiplies k, mimicking the stress. The dotted line indicates that the system does not display oscillatory behaviour.

out that the oscillations do not change qualitatively when the parameters a, b and c are varied (by up to five orders of magnitude), whereas a decrease in d or k_g suppresses the oscillating behaviour. Although no intuitive explanation for this behaviour has been found, it is interesting that these two critical parameters are associated with the delayed production of Mdm2. One could speculate therefore that these processes play an important role in the production of tumours that arise when the p53 response mechanism fails. This speculation is, in fact, consistent with the observation that around the 45% of all tumours display mutations in the p53 region which binds to DNA [45].

2.2. *Stability analysis of the p53–Mdm2 model*

The overall behaviour of the proteins with respect to time evidently depends on the parameters of the dynamic equations, that is the production and degradation rates and the delay. Over long timescales, the protein concentrations can either converge to a steady state or a limit cycle (i.e., sustained oscillations). Chaotic behaviour is never observed within this model.

A careful analysis of how the dynamics of the protein concentration depends on the parameters of the rate equations has been done by Neamtu and co-workers in [46]. The main conclusion of this work is that under the condition that the dissociation constant k between p53 and Mdm2 is small, there exists a critical delay, τ_0, above which the system shows oscillations (see details in appendix C).

In the language of dynamical systems, the transition when the delay, τ, crosses τ_0 is a Hopf bifurcation. A Hopf bifurcation is the generic type of bifurcation that occurs when a stable fixed point of the system becomes unstable and turns into a limit cycle, a dynamically oscillating state, as a consequence of a change in some parameter of the system (see appendix B for more details).

2.3. *Hes1 and its mRNA*

The transcription factor Hes1 controls the differentiation of neurons in mammalian embryos [47]. Its concentration is controlled by a feedback loop built out of Hes1 and its own mRNA (see figure 3). Like p53, its concentrations display oscillations when the cells are stimulated with serum [12]. The period is similar to that of p53, approximately 2 h, and the oscillations last for ≈12 h. Hes1 is known to repress another protein called Mash1. Both the knocking out of Mash1 and its continuous expression by means of retroviral introduction results in a lack of cell differentiation. Only when there are periodic oscillations in the concentration of Hes1 (and thus of Mash1) there is proper differentiation of neuronal cells [47], showing that the temporal variation of the protein concentrations is critical for the development of the nervous system.

The relation of Hes1 oscillations to segmentation and spatial patterns has been studied by several authors. It is well known that oscillations in Hes1 is part of Notch signalling and Hirata *et al* [12] studied the coordinated somite segmentation in the presomitic mesoderm of mice embryos and found a correlation between the oscillations of Hes1 and initiation of somites. The general issue of segmentation in vertebrates has been further studied in [13–15], indicating that the oscillations in the Notch pathway signalling are intimately related to the Wnt signalling. At the caudal end (i.e. the 'tail') of the embryo Notch and Wnt oscillates out of phase when the gradient in the Wnt level is over a given threshold [14, 15]. New cells are provided at the end of the embryo and where the Wnt level is below the threshold the oscillation stops and marks the boundary for a new somite. This continues until all somites are produced which subsequently gives rise to the spinal cord [13]. Ultradian oscillations of signalling pathways are thus extremely important for segmentation.

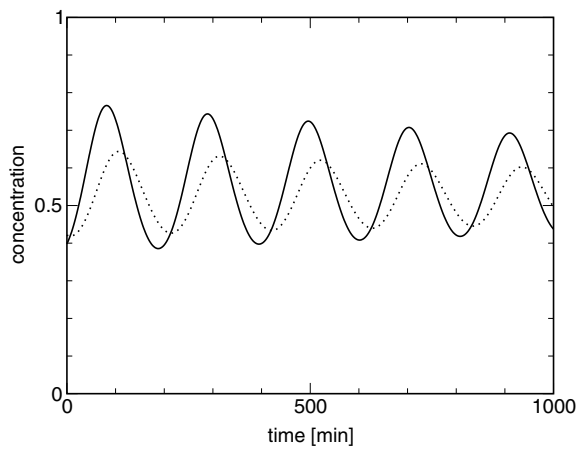

Figure 6. The concentration of Hes1 (solid curve) and of mRNA (dashed curve) obtained solving numerically equation (6).

The control mechanism of Hes1 oscillations again involves a negative feedback loop with one activation and one repression: the transcription of the mRNA of Hes1 activates the production (translation) of the protein, and Hes1 represses the transcription of its own mRNA. The main difference compared to p53 is that here one of the nodes represents an mRNA, not a protein. However, this difference is merely semantic: the control network still has two nodes, of which one is activating and one is repressing. The molecular species of these nodes are immaterial to the description of the oscillations[6].

We model the system using the following equations (cf [32]):

$$\frac{\mathrm{d}r}{\mathrm{d}t} = \frac{\alpha k^h}{k^h + [s(t-\tau)]^h} - k_r r(t)$$
$$\frac{\mathrm{d}s}{\mathrm{d}t} = \beta r(t) - k_s s(t), \qquad (6)$$

where s and r are the concentrations of Hes1 and its mRNA, respectively. The meaning of these equations is that mRNA is produced at a rate α when Hes1 is not bound to the DNA. The effect of binding Hes1 to DNA is to reduce the effective transcription rate. The probability that Hes1 is bound to DNA is $k^h/(k^h + s^h)$, where k is a characteristic concentration for dissociation of Hes1 from the DNA, and h is the Hill coefficient that takes into account the cooperative character of the binding process. k_r and k_s are the spontaneous degradation rates of the two proteins, while τ is the delay associated with the molecular processes that we do not want to describe explicitly (transcription, translocation, etc). [12] suggests that k_r^{-1} and k_s^{-1} are of the order of 25 min. The value of the time delay is difficult to assess, since it is determined by a combination of various molecular processes. One can guess that its order of magnitude is tens of minutes.

[6] We could of course introduce two more nodes in the p53 network representing the mRNA of p53 and Mdm2. However, this would not change the logic of the loop, replacing an activation by two successive activations. As discussed earlier, adding more intermediate nodes introduces a time delay. Since the p53 equations had an explicit delay it seems redundant to add the mRNA nodes also.

The numerical solution of equation (6) is displayed in figure 6. The oscillations have a period $\Delta\tau \approx 170$ min. For any delay in the range $10 < \tau < 50$ min, the oscillation period is consistent with that found experimentally, and so is the time difference between the peaks in Hes1 and mRNA, ≈18 min. For $\tau < 10$ min, the system shows no oscillations.

The behaviour of Hes1 is very similar to that of p53, both in the features of the oscillations and in the lag delay before they start. This is not unexpected, since the structure of equation (6) is very similar to the structure of equation (5) and to any time delay equation describing a two-component negative feedback loop.

2.4. NF-κB and IκB

The NF-κB family of proteins is one of the most studied in the last ten years, being involved in a variety of cellular processes, including immune response, inflammation, and development [3, 48]. NF-κB can be activated by a number of external stimuli [49] including bacteria, viruses and various stresses and proteins (for instance, [3, 7] used the tumour necrosis factor-α, TNF-α). In response to these signals it targets over 150 genes, including many chemokines, immunoreceptors, stress response genes, as well as acute phase inflammation response proteins [49]. Each NF-κB has a partner inhibitor called IκB, which inactivates NF-κB by sequestering it both in the nucleus as well as in the cytoplasm. In fact, the IκB proteins come in several isoforms α, β, ϵ [3, 50], and perhaps others [48]. Some of these isoforms are, in turn, transcriptionally activated by NF-κB, thus forming a negative feedback loop which is essentially identical in structure to the other two discussed above.

The potential for this negative feedback loop to produce oscillations in the nuclear–cytoplasmic translocation of NF-κB was initially shown by electrophoretic mobility shift assay experiments [3]. They found that wild-type cells and mutants containing only the IκBα isoform showed damped oscillations. In contrast, cells with only the IκBβ or ε isoforms do not show oscillations. This conclusion was bolstered by single-cell fluorescence imaging experiments which show sustained oscillations of nuclear NF-κB in mammalian cells [7], with a time period of the order of hours. In these experiments IκBα was overexpressed hence the system behaves like the mutant which has only the IκBα isoform.

As sustained oscillations are clearest here, we will focus our modelling on this mutant. The following cellular processes, summarized in figure 7, are important for this system on the timescales we are interested in (i.e., we ignore processes which are very slow):

- NF-κB, when in the nucleus, activates transcription of the IκBα gene (henceforth we will drop α unless we are explicitly talking about more than one isoform), producing IκB mRNA in the cytoplasm.
- The IκB mRNA is translated to form IκB protein.
- The IκB protein can be transported in and out of the nucleus.
- In both compartments, IκB forms a complex with NF-κB.

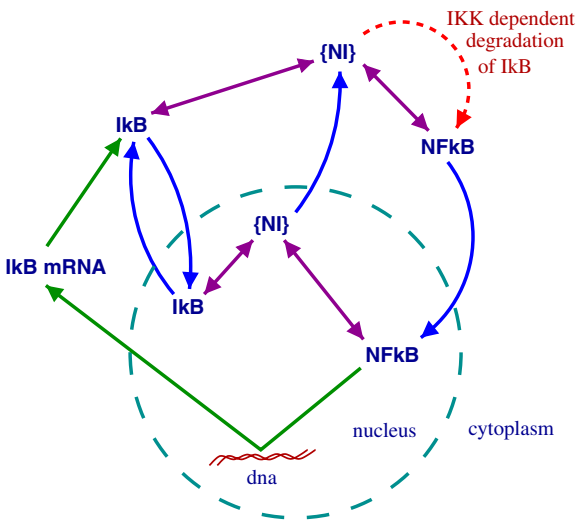

Figure 7. The important interactions in the NF-κB system. Green arrows indicate transcription and translation. Blue arrows indicate transport processes. Purple double arrows indicate complex formation. The red dashed arrow indicates IKK triggered degradation of IκB when complexed to NF-κB.

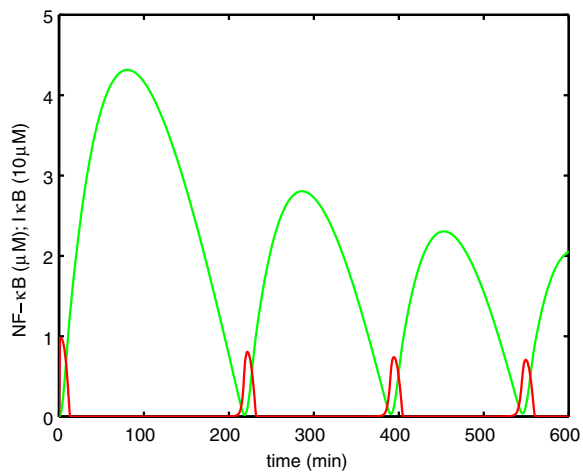

Figure 8. Oscillations of nuclear NF-κB (N_n), red, and cytoplasmic IκB, green, for $A = 0.007$, $B = 954.5$, $C = 0.035$, $\delta = 0.029$ and $\epsilon = 2 \times 10^{-5}$ (these parameter values are derived from those used in [3]; see [51].) In order to facilitate comparison with the experimental plot, the x-axis has been limited to 600 min, but the oscillations are in fact sustained (see figure 10(a)).

- The NF-κB-IκB complex (henceforth referred to as {NI}) cannot be imported into the nucleus. However, if it forms within the nucleus it can be exported out.
- Free NF-κB behaves in exactly the opposite way. Free NF-κB is actively transported into the nucleus but not from the nucleus to the cytoplasm.
- The cytoplasmic {NI} complex is tagged by another protein, the IκB kinase (IKK), for proteolytic degradation. This results in degradation of IκB only, releasing NF-κB. Note that this degradation does not occur for free IκB.

On the timescales of interest, there is no net production or degradation of NF-κB. It simply cycles in and out of the nucleus, i.e., the sum of nuclear and cytoplasmic NF-κB concentrations is a constant. Amongst the above-listed processes, the association and dissociation of the complex {NI} occurs fast enough that the concentration of the complex can be taken to be always in equilibrium with the free NF-κB and IκB concentrations. This allows us to describe the system using a very simple model consisting of only three variables [51], nuclear NF-κB (N_n), cytoplasmic IκB (I) and IκB mRNA (I_m):

$$\frac{\mathrm{d}N_n}{\mathrm{d}t} = A\frac{(1-N_n)}{\epsilon + I} - B\frac{IN_n}{\delta + N_n}, \tag{7}$$

$$\frac{\mathrm{d}I_m}{\mathrm{d}t} = N_n^2 - I_m, \tag{8}$$

$$\frac{\mathrm{d}I}{\mathrm{d}t} = I_m - C\frac{(1-N_n)I}{\epsilon + I}. \tag{9}$$

In these equations, all the variables and time have been rescaled so that they are dimensionless. The three-variable model was formed by reducing from a larger, seven-variable model which also kept track of the different complexes involving NF-κB and IκB (details of the larger model and the rescaling can be found in [51]).

The terms in equation (7) model the nuclear import and export of NF-κB. The import is inhibited by cytoplasmic IκB because it forms a complex with NF-κB which cannot enter the nucleus. Equation (8) models NF-κB-activated transcription of the IκBα gene (this term could also be modelled using a Michaelis–Menten term but we simplify it further following [3]) and spontaneous degradation of the mRNA. Finally, equation (9) has terms for translation of IκB mRNA into the protein and IKK mediated degradation of IκB. As the degradation occurs only on the {NI} complex, the dependence on IκB is of a Michaelis–Menten form. The external signal is supplied by IKK that enters the equations through the parameter, C, which is proportional to IKK concentration (this could also be converted into a Michaelis–Menten term, but at the cost of adding more parameters to the model).

These equations produce sustained oscillations in all variables over a wide range of parameter values. Figure 8 shows the result of simulations which use parameter values from [3]. The oscillations produced by this model match the experimentally observed features well, in particular, the shape, phase, time period and frequency response are correctly reproduced [51].

Note that this is certainly not the only model able to reproduce the experimental oscillations observed in NF-κB. Hoffman *et al* have constructed a long list of chemical reactions between 26 different molecules in the NF-κB system, including 65 numerical parameters [3, 50]. Hayot and Jayaprakash have also built a model with seven variables for NF-κB oscillations [52]. Another model, which is similar to Hoffman *et al*'s model, but has an additional feedback loop is described in [53].

2.5. *Saturated degradation of IκB*

A key element in the model is the saturated degradation of cytoplasmic IκB in the presence of IKK (second term in

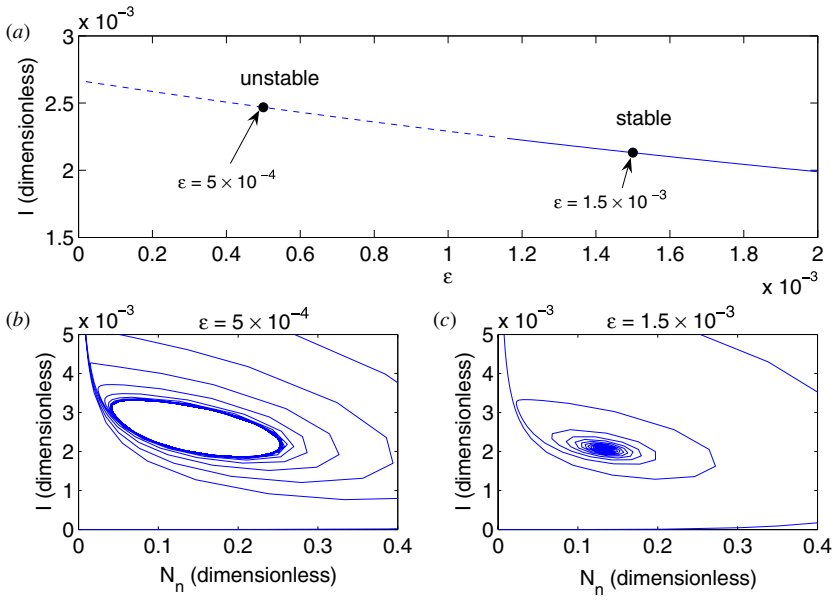

Figure 9. (*a*) The stationary value of I as a function of the parameter ϵ which controls the binding between NF-κB and IKK in the cytoplasm. (*b*) and (*c*) The projection of two trajectories at different values of ϵ onto the N_n–I plane. Note that a Hopf bifurcation takes place causing a stable fixed point (*c*) to bifurcate into a stable limit cycle (*b*).

equation (9)). This saturation occurs because the level of the NF-κB-IκB complex saturates, and this complex is needed for IKK triggered degradation of IκB. A stability analysis of the system shows the importance of the saturated degradation for oscillations. We begin by examining the fixed points of the system.

The fixed point values of N_n, I_m and I are solutions to

$$A\frac{(1-N_n)}{\epsilon+I} - B\frac{IN_n}{\delta+N_n} = 0,$$
$$N_n^2 - I_m = 0,$$
$$I_m - C\frac{(1-N_n)I}{\epsilon+I} = 0.$$

I_m and I can be eliminated using $I_m = N_n^2$, giving $I = \left(N_n^2\epsilon\right)/\left(C - CN_n - N_n^2\right)$. From this we find that the fixed point value of N_n is a solution of the equation $\left(C - CN_n - N_n^2\right)^2 = \left(BC\epsilon^2 N_n^3\right)/[A(\delta+N_n)]$, or equivalently,

$$N_n^5 + (\delta+2C)N_n^4 + C\left[2(\delta-1) + C - \frac{B}{A}\epsilon^2\right]N_n^3$$
$$+ C[(C-2)\delta - 2C]N_n^2 + C^2(1-2\delta)N_n + C^2\delta = 0.$$

In general, this has two real solutions, one with $C - CN_n - N_n^2 > 0$ and the other with $C - CN_n - N_n^2 < 0$. The latter results in a negative value for I and therefore is not an acceptable solution. Thus we are left with only one fixed point.

Next we linearize the system around the fixed point, which we denote N^*, I_m^*, I^*, and thereby obtain the Jacobian matrix. Formally writing the three equations as follows,

$$\begin{pmatrix} \dot{N} \\ \dot{I}_m \\ \dot{I} \end{pmatrix} = \begin{pmatrix} f(N, I_m, I) \\ g(N, I_m, I) \\ h(N, I_m, I) \end{pmatrix} \tag{10}$$

we can write the Jacobian:

$$J = \begin{pmatrix} \frac{\partial f}{\partial N} & \frac{\partial f}{\partial I_m} & \frac{\partial f}{\partial I} \\ \frac{\partial g}{\partial N} & \frac{\partial g}{\partial I_m} & \frac{\partial g}{\partial I} \\ \frac{\partial h}{\partial N} & \frac{\partial h}{\partial I_m} & \frac{\partial h}{\partial I} \end{pmatrix}_{N^*, I_m^*, I^*} \tag{11}$$

For our NF-κB model this gives

$$J = \begin{pmatrix} -\frac{A}{\epsilon+I} - \frac{\delta BI}{(\delta+N_n)^2} & 0 & -\frac{A(1-N_n)}{(\epsilon+I)^2} - \frac{BN_n}{\delta+N_n} \\ 2N_n & -1 & 0 \\ \frac{CI}{\epsilon+I} & 1 & -\frac{C\epsilon(1-N_n)}{(\epsilon+I)^2} \end{pmatrix}.$$

This matrix can be used to examine the stability of the fixed point: it is unstable if any of the eigenvalues has a positive real part. For the NF-κB system, figure 9 shows how the stability depends on the parameter ϵ. When ϵ is small compared to the steady state value of I, the degradation rate of IκB is independent of I, which is what we mean by the term 'saturated degradation'. On the other hand, when ϵ is large then the degradation is proportional to I and is not saturated. Figure 9 shows that, indeed, the fixed point is unstable when ϵ is small compared to I and through a Hopf bifurcation the fixed point is replaced by a stable limit cycle. Physically, this is because saturated degradation introduces an effective time-delay into the feedback loop: it allows IκB to accumulate and stay around longer than with non-saturated degradation.

2.6. *Spikiness and sharp response of the NF-κB oscillation*

One property of the oscillations of nuclear NF-κB, in figure 8, that stands out is that they are extremely spiky. By choosing different parameter values one can also get soft oscillations (see figures 10(*a*) and (*b*)); however, for biologically relevant

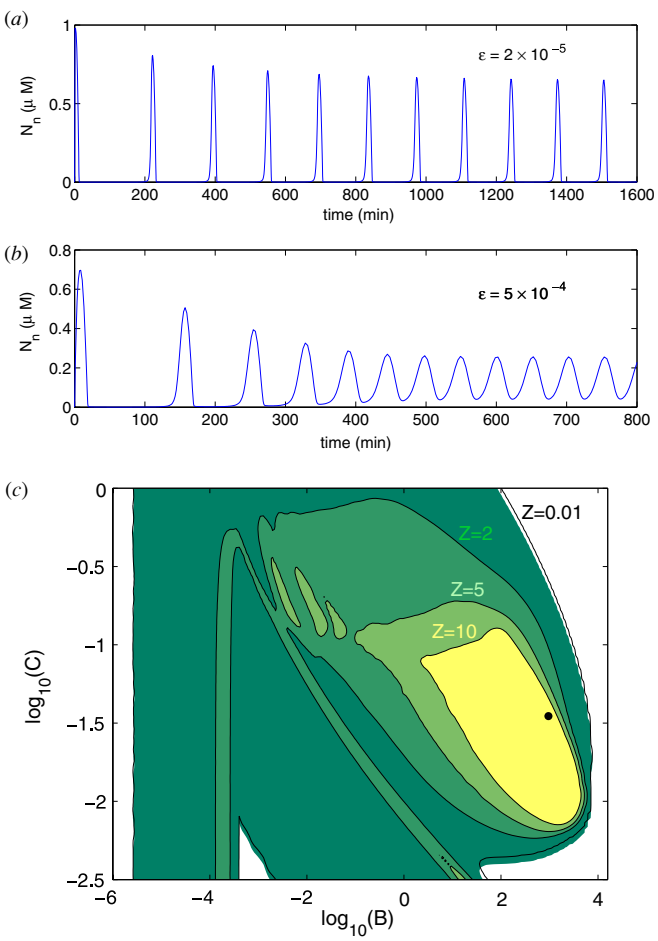

Figure 10. (*a*) Spiky oscillations in the NF-κB model (parameter values are identical to those used to produce figure 8). (*b*) Soft oscillations, produced in the same model using a larger value of ϵ, keeping all other parameters unchanged. (*c*) A contour plot of the Z measure of spikiness (see text), in the B–C parameter plane (other parameters are unchanged). The $z = 0.01$ contour maps, approximately, the region of oscillations. The $Z = 2$ contour shows the region of spiky oscillations. The black dot marks the value of B and C used in (*a*) and (*b*), as well as in figure 8.

parameters the oscillations are spiky. We suggest the following measure of spikiness:

$$Z = \frac{\max - \min}{\text{average}}. \tag{12}$$

In other words, Z is the ratio of the amplitude of the oscillations to the average level. Then, we will call a particular oscillation *spiky* if $Z > 2$ and *soft* otherwise. Further, $Z = 0$ indicates the absence of oscillations. Figure 10(*c*) shows a contour plot of Z values on the B–C plane. In some directions the system transitions quickly from no oscillations to spiky oscillations, whereas in other directions there is a softer transition. In general, the existence and spikiness of the oscillations are very robust to changes in most of the parameters of the model [51].

There is one parameter, however, to changes in which the system shows a very sensitive response. That parameter is the external input, IKK. Figure 11 shows that both the spike height (or peak level), as well as the spike duration, can change by large amounts in response to small changes in IKK level. Note that this sensitivity is particularly high in IKK ranges which are near the transition from spiky to soft oscillations. One way of quantifying this sensitivity is to measure the expression level of a gene whose transcription is activated by NF-κB. Imagine a gene whose upstream regulatory region contains a binding site for NF-κB dimers. Upon binding, the gene promoter is activated: $G + 2N \underset{k_{\text{off}}}{\overset{k_{\text{on}}}{\rightleftharpoons}} G^*$. Experimental measurements of NF-κB-dependent gene expression suggest that many genes closely follow the oscillations of NF-κB [8]. This corresponds to the case where the binding of NF-κB to the operator is in equilibrium, i.e., k_{on} and k_{off} are much larger than the rates of all other processes in the NF-κB system. In that case the gene activity, G^*, will follow the NF-κB concentration: $G^* = \frac{N_n^2}{k_{\text{off}}/k_{\text{on}} + N_n^2}$. In this case the downstream gene inherits the high sensitivity of the NF-κB signal to IKK: the peak gene activity as a function of IKK is a very steep sigmoidal curve with an effective Hill coefficient of over 20 [51]. Such a large value is very unusual for biological systems, and is much larger than the values obtained by other mechanisms [54, 55].

3. A tool to analyse oscillation patterns in time series

After having discussed the mechanism underlying the production of oscillations and studied in detail three examples of 'ultradian' oscillations in cells, we would like to describe an easy tool [56] capable of providing information on the architecture of the underlying network, given the experimental time series data for oscillating biological systems.

More precisely, given the time sequence of maxima and minima of the concentrations of the species during the oscillations, the method allows one to assess whether the observed sequence is compatible with a single underlying negative feedback loop, describable by equation (2). If it is, the method further predicts the logical structure of the loop, i.e. the order of the proteins within the loop, as well as which protein acts as an activator and which as a repressor.

The method is grounded in a mathematical result valid for all monotone systems describable by equation (2). For such a system, we can prove the following statements about the sequence of maxima and minima in the time series:

- the extrema (maxima or minima) have to follow the order of the variables; for example, after a maximum of variable $i - 1$ there can either be a maximum or a minimum of variable i, and
- if two successive extrema are of the same kind (both maxima, or both minima), then variable i is activated by variable $i - 1$. Conversely, if they are of opposite nature (one maximum and one minimum), then variable i is repressed by variable $i - 1$.

These statements can be used to reconstruct the structure of the underlying loop from the time series, if it is compatible with the above restrictions. We illustrate this using the example of p53-Mdm2 time series shown in figure 12. The reconstructed loop is exactly the structure we used in equation (5): p53 activates Mdm2, which represses p53. Of course, in this case, there are only two possible loop structures,

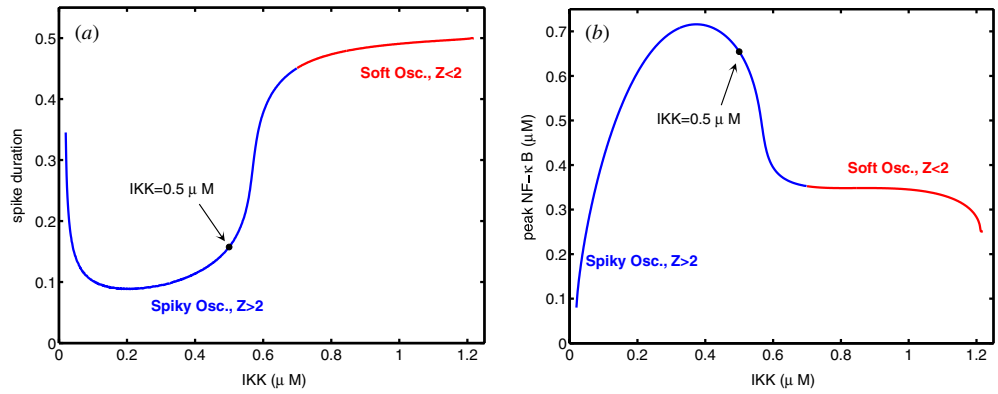

Figure 11. Sensitivity to IKK. (*a*) Spike duration, the fraction of time N_n spends above its mean value, as a function of IKK concentration. (*b*) Spike peak, the maximum concentration of nuclear NF-κB, as a function of IKK concentration. In both plots, the black dot shows the IKK value used in figure 8, while blue and red signify, respectively, regions of spiky and soft oscillations.

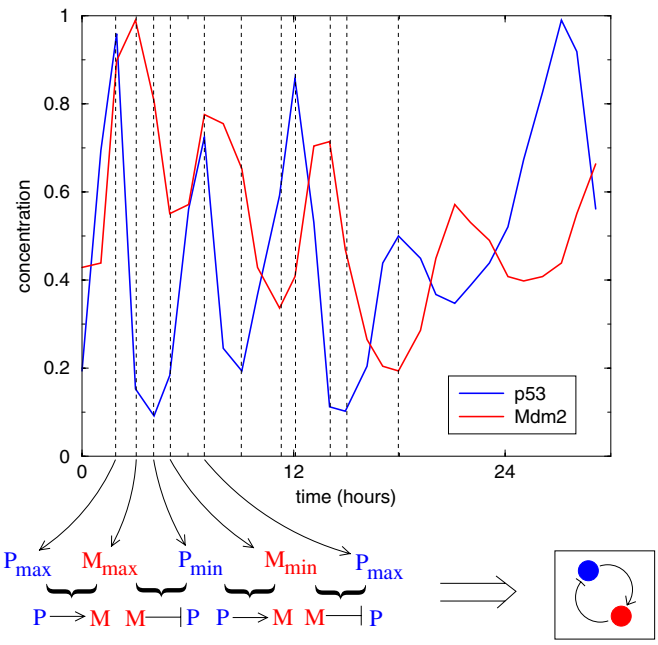

Figure 12. Reconstructing the underlying loop from the time series. The time series shows p53-Mdm2 oscillations observed in single cell fluorescence experiments [6]. Using the rules mentioned in the text, the sequence of maxima and minima is converted to the feedback loop shown at bottom right.

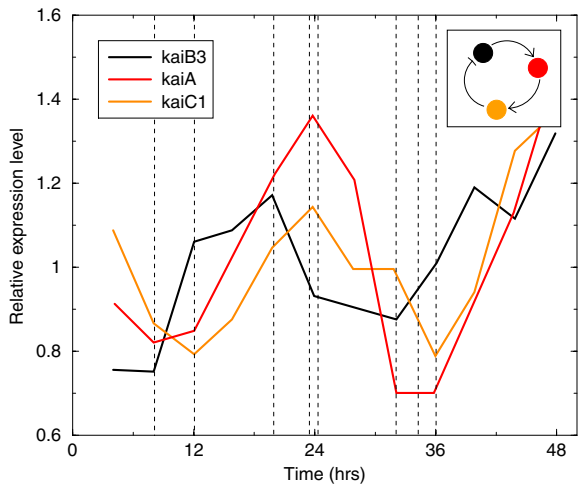

Figure 13. Reconstruction algorithm applied to circadian rhythms in cyanobacteria. Data from [10]. The algorithm predicts that *kaiA* activates *kaiC1*, which represses *kaiB3*, which, in turn, activates *kaiA*.

and the correct interactions are already known experimentally so the information gained is minimal. The method comes into its own for systems with more variables. One example is the cyanobacterial circadian clock. Figure 13 shows oscillations in the expression of three circadian clock genes in *Synechocystis* and the reconstructed loop. Two of the interactions have been experimentally observed in another strain of cyanobacteria [57], but the activation of *kaiA* by *kaiB3* is a new prediction.

Note that there are many possible maxima/minima sequences which are not compatible with the above rules. For example, in order to be compatible with a single loop, each species must have exactly one maximum and one minimum during one period. Moreover, if the method predicts an even number of repressors, one should consider an oscillating positive feedback loop, which is impossible (see [56] for a full list of non-allowed cases). In all these situations, one should conclude that the mechanism causing the oscillations is more complicated and cannot be reduced to a single feedback loop. Even if the structure of the real protein interaction network is more complicated that a single loop (which is usually the case), the method can hint at the interactions which are most relevant for the oscillating mechanism and help in building up a zeroth-order model of the system.

Finally, we note that while the method is mathematically rigorous for systems without time delays, it works even if there are unobserved chemical species taking part to the loop [56]. As intermediate species introduce time delays it is likely that the result can be extended to systems with an explicit time delay added to equation (2).

4. Summary and outlook

Questions about cellular processes that use complex, temporally varying signals can be crudely classified into

the 'how' and 'why' groups. 'How' questions deal with the structure of the regulatory network and the range of dynamical behaviour it can produce: how does the network produce oscillations? what are the necessary and sufficient mechanisms? how are they implemented in real cellular systems? 'Why' questions deal with the physiological role of the particular dynamical behaviour produced by the network: why does p53 start oscillating in response to DNA damage? do oscillations carry some information that can be decoded by downstream genes? could a non-oscillating system have worked equally well for the cell?

In this review we have mainly investigated the 'how' questions for one subset of cellular response systems that use temporally varying signals: eukaryotic systems exhibiting 'ultradian' oscillations. The three systems we have modelled—p53, which is important for apoptosis, Hes1, which is part of the Notch cycle responsible for somite segmentation, and NF-κB, a key protein in immune response—all turn out to have the same basic design that produces oscillations. The two key aspects of this design are the presence of *negative feedback* and *time delays*. There are many ways of producing an effective time delay in cellular processes. In particular, we emphasized, using the example of NF-κB, *saturated degradation* as one such mechanism.

Saturated degradation plays a role in many models of oscillatory negative feedback loops. The earliest use of this mechanism is in the model of Bliss, Painter and Marr [36], which is similar to our NF-κB model. Saturated degradation has also been used by Goldbeter in various models of cellular oscillations, e.g., the cell cycle [58], development in myxobacteria [59], yeast stress response [60] and the mammalian circadian clock [61]. It is also found in models of calcium oscillations in cells [62, 63]. In the p53-Mdm2 system too, as described earlier, there is a similar saturated complex formation, where one component of the complex is subsequently degraded. This is so similar to the NF-κB case that it should be possible to construct a model for p53 oscillations which has ordinary differential equations without an explicit time delay (see, for instance, [6]). Because saturated degradation is easily implemented by complex formation we conclude that it would be a very useful general mechanism for producing an effective time delay in cellular systems.

Although we have focussed more on how the oscillations are produced, the 'why' question of whether the oscillations have a direct physiological role in these systems is of course an important one. In NF-κB, oscillations are observed, not in wild-type cells, but rather in mutants or cells which overexpress certain proteins. Therefore, it is quite possible that oscillations themselves play no direct role in the wild-type response [64]. However, wild-type cells do show a complex temporal variation of NF-κB of which the spiky response of the IκBα module is an extremely important component (IκBα is the only isoform whose knockout mutants are not viable [3]). Hes1 oscillations, even though damped, might have a direct relevance for spatial pattern formation in embryos. Hes1 is a key element in the Notch oscillating cycle, which, in mouse and chicken embryos, is coupled, out of phase, with the Wnt cycle. In each period of these cycles, a somite is formed, thus leading to vertebrate segmentation. Further work should clarify whether the Hes1 oscillations drives these cycles, or is slaved to them, or has a different role entirely. In the case of p53, the oscillations appear to be sustained; therefore it is likely they are directly important for the apoptosis pathway, but again it is not clear precisely how.

Even in the absence of unambiguous evidence that oscillations have a direct functional importance, investigations into the mechanisms underlying the oscillations have implications for some of the 'why' questions. For instance, noting that an oscillating signal carries much more information than a steady signal, references [17, 65] suggested that differential regulation of downstream gene circuits could be achieved if they were sensitive to the frequency of the oscillation. Indeed, as we have shown [51], it is easy for a single downstream gene to act as a 'low-pass filter'. Regulatory circuits with multiple genes could be constructed to have particular frequency responses. However, it is perhaps more fruitful to look for a physiological role in other properties of the dynamics, rather than the periodicity. One such property, especially prominent in NF-κB oscillations, is the spikiness. A spiky signal of this kind carries even more information than a soft oscillation or a steady state level. Spiky pulses, whether periodic or random or isolated, are in a sense less 'expensive': if a downstream gene is expressed when p53 crosses some threshold it is energetically and metabolically cheaper to have a spike whose peak crosses the threshold for long enough to trigger the gene, than to produce and maintain the protein above that level for a long time.

In this context it is noteworthy that several of the most ubiquitous signalling molecules in eukaryotes, hormones, exhibit recurrent spikes. The spikes sometime come in a nearly periodic fashion but may also appear more randomly. Why hormones appear in spikes is also not known. Again, we speculate that spikes are an efficient way to trigger other regulatory mechanisms in the body as compared to a steady level which does not deliver 'kicks' to stimulate other compartments. An added benefit is that the time between spikes allows an extra level of regulation. In addition, it might not be good for a biological organism to be subjected to a constant level of hormones all around the clock.

A related issue where spikiness has implications is that of cross-talk between signals. Thus, a high constant level of a protein may potentially interfere with other signals being sent, for instance by saturating common receptors. In contrast, a 'quantization' of the signal into spikes allows different signals to use common receptors without fear of interference. An analogy to cars is perhaps useful to visualize this difference: If there were no traffic lights, it would still be easy to drive a car to your destination provided the traffic was not too heavy. However, if all cars were made 10 times longer it would become much harder to drive at the same density of traffic. Indeed, railway tracks have less intersections because trains are, in effect, very long cars.

On a more concrete level, our analysis of the NF-κB network suggests that the spikiness of the oscillations was correlated to a sharp, threshold-like response of the system.

The output (nuclear NF-κB concentration), we found, could be extremely sensitive to changes in the input (IKK) while remaining relatively insensitive to other parameters—a clear prediction that awaits experimental verification. Such a threshold-like response is likely to be very important for the differential regulation of downstream genes. It would be very interesting to know if there is a causal connection between spikiness and sharp responses in this system, as well as other regulatory systems.

Overall, we conclude that oscillations, especially spiky ones, have many useful properties that could be exploited to improve the speed and efficiency of signalling and response systems.

Acknowledgments

We are grateful to Alexander Hoffmann, Terry Hwa, Arnie Levine, Eric Siggia, Galit Lahav and Ian Dodd for interesting discussions on oscillating genetics. SK, MHJ and KS acknowledge support from the Danish National Research Foundation and Villum Kann Rasmussen Foundation. GT acknowledges support from the FIRB 2003 program of the Italian Ministry for University and Scientific Research.

Appendix A. Properties of monotone systems

In this section we study the fixed point properties of a feedback loop composed of an arbitrary number, N, of nodes whose dynamics is given by equation (2) in the main text, which we repeat here:

$$\frac{\mathrm{d}x_i}{\mathrm{d}t} = g_i^{(A,R)}(x_i, x_{i-1}) \qquad i = 1, \ldots, N. \tag{A.1}$$

Our analysis proceeds by noting that, using the monotonicity condition, we can write explicit functional relations between neighbouring variables in the steady state (when $\mathrm{d}x_i/\mathrm{d}t = 0$):

$$g_i^{(A,R)}(x_i^*, x_{i-1}^*) = 0 \quad \Rightarrow \quad x_i^* = f_i^{(A,R)}(x_{i-1}^*). \tag{A.2}$$

Note that the functions f_i have the same monotonicity properties as the g_is with respect to the second argument (for this it is necessary that $g_i(x, y)$ be a monotonically *decreasing* function of x). By iterative substitution, we obtain

$$\begin{aligned} x_i^* &= f_i(x_{i-1}^*) = f_i(f_{i-1}(x_{i-2}^*)) = \cdots = \\ &= f_i \circ f_{i-1} \circ f_{i-2} \circ \ldots \circ f_{i+1}(x_i^*) \equiv F_i(x_i^*) \end{aligned} \tag{A.3}$$

where $\circ$ denotes convolution of functions. Here, we introduced the function $F_i(x)$, which quantifies how the species i interacts with itself by transmitting signals along the loop. Note also that if equation (A.3) holds for one value of i, then it holds for any i, since it is sufficient to apply $f_{i+1}()$ on both sides to obtain the equation for x_{i+1}^* and so on. For feedback loops, much useful information can be obtained from the properties of $F_i(x)$. Firstly, by applying the chain rule, we obtain the slope of $F_i(x)$ at x: $F_i'(x) = \prod_j f_j'(x_j)|_{x_i=x}$. The r.h.s is always greater (less) than zero if the number of repressors present in the loop is even (odd). In the former case, there can be multiple fixed points, i.e., this is a necessary condition for multistability. On the other hand, when there are an odd number of repressors, then $F_i(x)$ is positive and monotonically decreasing, meaning that there is one and only one solution to the fixed point equation $x_i^* = F_i(x_i^*)$.

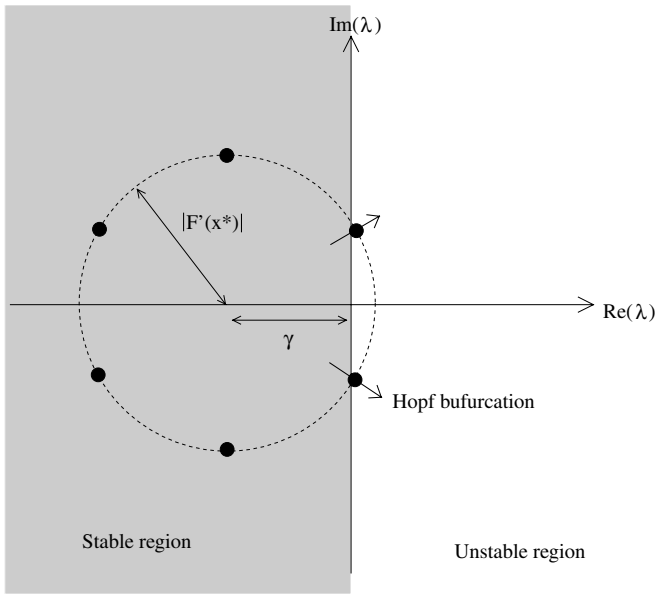

Figure 14. Sketch of the Hopf bifurcation in the eigenvalue complex plane, in the case in which all the degradation rates are equal to a constant γ.

To perform the stability analysis, we write the characteristic polynomial evaluated at the fixed point:

$$\prod_i [\lambda - \partial_x g_i(x, y)|_{x=x^*}] = \prod_i \partial_y g_i(x, y)|_{x=x^*}. \tag{A.4}$$

The above equation can be greatly simplified using the relation $F'(x) = \prod_i \partial_y g_i(x, y)/\partial_x g_i(x, y)$, which is a consequence of the implicit function theorem and the chain rule. One then obtains the following equation:

$$\prod_{i=1}^{N} \left(\frac{\lambda}{h_i} + 1 \right) = F'(x^*) \tag{A.5}$$

where the $h_i = -\partial_x g_i(x_i, x_{i=1})|_{x^*}$ are the degradation rates at the fixed point. Note that, because $F'(x)$ is always negative in a negative feedback loop, all coefficients of the characteristic polynomial are non-negative, hence it can not have real positive roots. This means that the destabilization of the fixed point can only occur via a Hopf bifurcation, i.e. with two complex conjugate eigenvalues crossing into the positive real half-plane.

In the simple case in which all the degradation rates are equal and unchanging (i.e, $h_i = \gamma$, a constant) the roots of the polynomial (A.5) in the complex plane are the vertices of a polygon centred on $-\gamma$ with a radius $|F'|$ as sketched in figure 14.

Therefore, the fixed point will remain stable as long as

$$|F'(x^*)| \cos(\pi/N) < \gamma. \tag{A.6}$$

In this case, Hopf's theorem (see appendix B) ensures the existence of a periodic orbit close to the transition value, whose period is

$$T = 2\pi/\mathrm{Im}(\lambda) \tag{A.7}$$

which, in the simple case of equal degradation timescales, becomes $T = 2\pi/[|F'(x^*)| \cdot \sin(\pi/N)]$. Note that the Hopf theorem does not ensure that the orbit is stable; however, since the system is bounded and there are no other fixed points, we expect the orbit to be attracting, at least close to the transition point.

Note that condition (A.6) is always satisfied when $N = 2$. This result also extends to the more general case where degradation rates are unequal. Thus, we have proven that a two-component monotone negative feedback loop without an explicit time delay can never show oscillations.

Appendix B. Hopf bifurcations

Usually, the bifurcation takes place under the variation of some external 'control' parameter μ and the new state appears at a critical value μ_c of this parameter. For genetically regulated networks, the control parameter could be some external chemical stimuli, a production rate, or a binding constant, just to mention a few examples. To illustrate a Hopf bifurcation let us first consider a completely general two-dimensional dynamical system (without delay) defined by two coupled nonlinear differential equations

$$\begin{pmatrix} \dot{p} \\ \dot{m} \end{pmatrix} = \begin{pmatrix} f(p,m) \\ g(p,m) \end{pmatrix} \tag{B.1}$$

(we use variables (p, m) to resemble p53 and mdm2). The stationary fixed point (p^*, m^*) is determined by

$$f(p^*, m^*) = g(p^*, m^*) = 0. \tag{B.2}$$

Using standard routines one linearizes around the fixed point by means of the Jacobian matrix

$$J = \begin{pmatrix} \frac{\partial f}{\partial p} & \frac{\partial f}{\partial m} \\ \frac{\partial g}{\partial p} & \frac{\partial g}{\partial m} \end{pmatrix}_* \tag{B.3}$$

where the star symbolizes that we insert the fixed point into the Jacobian. The resulting set of eigenvalues λ_1, λ_2 can either both be real or be a set of two complex conjugates. This is the case we are interested in here:

$$\lambda_1 = \alpha + \mathrm{i}\omega, \qquad \lambda_2 = \alpha - \mathrm{i}\omega. \tag{B.4}$$

For $\alpha < 0$ (corresponding to $\mu < \mu_c$) the fixed point (p^*, m^*) is stable whereas the limit cycle becomes stable for $\alpha > 0$ (corresponding to $\mu > \mu_c$) and performing oscillations on the limit cycle with a frequency ω defining the period of the oscillation. For a genetic system, this period could for instance be circadian, ultradiand or related to cell cycles. Just above the bifurcation, the limit cycle can be well approximated by a circle whose radius for super-critical Hopf bifurcations generally grows continuously as $\sqrt{\mu - \mu_c}$ (as in contrast to a sub-critical Hopf bifurcation where the radius will jump and exhibit hysteresis effects). When the control parameter μ is much larger than μ_c, the limit cycle may easily be deformed in various ways 'away' from the circle.

When we introduce a time delay in the equations, as discussed above, we can formally write it by introducing the delayed variable p_τ into the equations:

$$\begin{pmatrix} \dot{p} \\ \dot{m} \end{pmatrix} = \begin{pmatrix} f(p,m) \\ g(p,m,p_\tau) \end{pmatrix}. \tag{B.5}$$

We find numerically that the system still exhibits Hopf bifurcations when crossing critical lines in the parameter space. In fact, we find that one can drive the system through Hopf bifurcations by increasing the value of the time delay τ through specific values.

The fixed point of p is of course equal to the fixed point of p_τ, i.e., $f(p^*, m^*) = g(p^*, m^*, p^*) = 0$. Now we use the same approach as above and linearize around the fixed point,

$$q = p - p^*, \quad r = m - m^*, \quad q_\tau = p_\tau - p^*, \tag{B.6}$$

which leads to the following dynamical equations for the increments:

$$\begin{aligned} \dot{q} &= f(p^* + q, m^* + r) = f(p^*, m^*) + \frac{\partial f}{\partial p} \cdot q + \frac{\partial f}{\partial m} \cdot r \\ &= 0 + \alpha \cdot q + \beta \cdot r \end{aligned} \tag{B.7}$$

$$\begin{aligned} \dot{r} &= g(p^* + q, m^* + r, p^* + q_\tau) \\ &= g(p^*, m^*, p^*) + \frac{\partial g}{\partial p} \cdot q + \frac{\partial g}{\partial m} \cdot r + \frac{\partial g}{\partial p_\tau} \cdot q_\tau \\ &= 0 + \gamma \cdot q + \delta \cdot r + \epsilon \cdot q_\tau. \end{aligned} \tag{B.8}$$

We can now assume solutions on the form

$$q(t) = q_1 \mathrm{e}^{\lambda_1 t} + q_2 \mathrm{e}^{\lambda_2 t}, \qquad r(t) = r_1 \mathrm{e}^{\lambda_1 t} + r_2 \mathrm{e}^{\lambda_2 t}, \tag{B.9}$$

and find after some lengthy algebra the eigenvalues:

$$\lambda_1 = \tfrac{1}{2}\left[\alpha + \delta \pm ((\alpha - \delta)^2 + 4\beta(\epsilon\, \mathrm{e}^{-\lambda_1 \tau} + \gamma))^{\frac{1}{2}}\right] \tag{B.10}$$

$$\lambda_2 = \tfrac{1}{2}\left[\alpha + \delta \pm ((\alpha - \delta)^2 + 4\beta(\epsilon\, \mathrm{e}^{-\lambda_2 \tau} + \gamma))^{\frac{1}{2}}\right]. \tag{B.11}$$

We note that these are transcendental equations in the eigenvalues λ_1, λ_2 but that the time delay τ specifically appears into the relations (for a further discussion, see the previous appendix).

In many biological systems with genetic feedback regulations, there are often more than two dynamical variables, for instance the NF-κB system discussed earlier. The procedure to study this type of equations is exactly the same as for the two-dimensional system. In this case one obtains three eigenvalues $\lambda_1, \lambda_2, \lambda_3$ which are either all three real, or one is real and the two others complex conjugates. Again, in the last case one may encounter a Hopf bifurcation where the fixed point bifurcates into a limit cycle in the three-dimensional configuration space, causing oscillations in these variables. Note that there topologically is a big difference between oscillatory limit cycles in two and three dimensions. In two dimensions a limit cycle can 'enclose' trajectories, which is not the case in three dimensions where trajectories may 'escape around' the limit cycles. An important theorem for this type of behaviour is called the Poincare–Bendixson theorem, which states that if a trajectory is confined to a closed, bounded region and there are no fixed points in that region, then the trajectory eventually approaches a closed orbit (see, e.g., [28]).

Appendix C. Stability analysis of delay systems

Appendix C.1. Linear delay systems

Consider the simplest delayed system of the form

$$\frac{\mathrm{d}x}{\mathrm{d}t} = ax(t) + bx(t - \tau). \tag{C.1}$$

A complete description of the solution is given in an appendix of [66], while we will just investigate the conditions where the system display sustained oscillations. The general solution of equation (C.1) is $x = \exp(\lambda t)$ which, inserted in t investigate the conditions where the system display sustained oscillations. The general solution of equation (C.1) gives

$$\lambda = a + b\,\mathrm{e}^{-\lambda\tau}. \tag{C.2}$$

Defining $\lambda = \mu + \mathrm{i}\omega$, the oscillatory case takes place when $\mu = 0$. The solution is then

$$\mathrm{i}\omega = a + b\cos\omega\tau - \mathrm{i}b\sin\omega\tau \tag{C.3}$$

which gives

$$\omega = (b^2 - a^2)^{1/2} \tag{C.4}$$

$$\tau = \frac{\arccos(-a/b)}{(b^2 - a^2)^{1/2}}. \tag{C.5}$$

A more general treatment [67] gives the conditions under which the system converges to a stationary solution, that is $|a| > |b|$ for any τ or if $|a| < |b|$ for $\tau < \arccos(-a/b)/((b^2 - a^2)^{1/2})$. Roughly speaking, the system can oscillate if the dominant part of the kernel is the delayed one and if the delay is large enough.

Appendix C.2. Absence of closed orbits

If we label the vector forming the left-hand side of equation (1) as $\mathbf{x}$ and that forming the right-hand side as $\mathbf{F}$, its divergence of $\mathbf{F}$ is

$$\nabla\cdot\mathbf{F} = \frac{\partial g_1}{\partial x_1} - k_x + \frac{\partial g_2}{\partial x_2} - k_y. \tag{C.6}$$

Since we exclude that each of the two molecules can activate itself, the partial derivatives $\partial g_1/\partial x_1$ and $\partial g_2/\partial x_2$ are non-positive, and consequently $\nabla\cdot\mathbf{F} \leqslant 0$. By virtue of Green's theorem, if the trajectory C were closed,

$$0 > \int \nabla\cdot\dot{\mathbf{x}}\,\mathrm{d}A = \oint_C \dot{\mathbf{x}}\cdot\mathbf{n}\,\mathrm{d}l, \tag{C.7}$$

where $\mathbf{n}$ is the normal to the trajectory, and consequently $\dot{\mathbf{x}}\cdot\mathbf{n} = 0$ everywhere. Since the circulation of a null vector is zero, this leads to a contradiction, and the trajectory cannot be closed.

Appendix C.3. Stability analysis of the p53-mdm2 system

Neaumtu and co-workers develop in [46] the complete stability analysis of the p53-mdm2 system with delay. First they show that for any choice of the parameters there is a unique stationary point for the rate equations. Consider the system obtained by linearization of equation (5) around such point

$$\begin{aligned}\frac{\mathrm{d}p}{\mathrm{d}t} &= (a\rho_{10} - b)p(t) - a\rho_{01}m(t)\\ \frac{\mathrm{d}m}{\mathrm{d}t} &= -dm(t) + c\gamma_{10}p(t-\tau) + c\gamma_{01}p(t-\tau),\end{aligned} \tag{C.8}$$

where ρ_{10} and ρ_{01} are the derivatives of $r(t)$ with respect to p and m in the stationary point, while γ_{10} and γ_{10} are the derivatives of the function $p - r/(k_g + p - r)$. Define $p_1 = b + d + a\rho_{10}$, $p_0 = db + ad\rho_{10}$, $q_1 = c\gamma_{01}$ and $q_0 = c\gamma_{01}(b + a\rho_{10}) - ac\rho_{01}\gamma_{10}$. Let λ be the eigenvalues of the linearized system. It is possible to prove that if $\tau > 0$ and $p_1^2q_0^2 - q_1^2p_0^2 - 2p_0q_0^2 > 0$ then there is a delay τ_0 such that

$$\mathrm{Re}\left(\frac{\mathrm{d}\lambda}{\mathrm{d}\tau}\right)_{\lambda=\mathrm{i}\omega_0,\tau=\tau_0} > 0 \tag{C.9}$$

and consequently a Hopf bifurcation occurs at the stationary point.

In the limit of large dissociation constant k, $\rho_{10} = \rho_{01} = 0$. Consequently the condition for a Hopf bifurcation begins $b^2 > 0$, which is always satisfied (except for the trivial case $b = 0$).

The critical delay τ_0 is given by

$$\tau_0 = \frac{1}{\omega_0}\left(\arcsin\frac{p_1\omega_0}{\sqrt{\left(p_0 - \omega_0^2\right)^2 + \omega_0^2p_1^2}} + \arcsin\frac{q_1\omega_0}{\sqrt{\left(p_0 - \omega_0^2\right)^2 + \omega_0^2p_1^2}}\right), \tag{C.10}$$

where ω_0 is the solution of the equation

$$\omega^4 + \left(-p_1^2 - 2p_0 + q_1^2\right)\omega^2 + p_0^2 - q_0^2 = 0. \tag{C.11}$$

References

[1] Little J W 1983 The SOS regulatory system: control of its state by the level of RecA protease *J. Mol. Biol.* **167** 791–808

[2] Sassanfar M and Roberts J W 1990 Nature of the SOS-inducing signal in Escherichia coli: the involvement of DNA replication *J. Mol. Biol.* **212** 79–96

[3] Hoffmann A, Levchenko A, Scott M L and Baltimore D 2002 The IkappaB-NF-kappaB signaling module: temporal control and selective gene activation *Science* **298** 1241–5

[4] Yamamoto T, Nakahata Y, Soma H, Akashi M, Mamine T and Takumi T 2004 Transcriptional oscillation of canonical clock genes in mouse peripheral tissues *BMC Mol. Biol.* **5** 18

[5] Lahav G, Rosenfeld N, Sigal A, Geva–Zatorosky N, Levine A J, Elowitz M B and Alon U 2004 Dynamics of the p53–Mdm2 feedback loop in individual cells *Nat. Genet.* **36** 147–50

[6] Geva-Zatorsky N *et al* 2006 Oscillations and variability in the p53 system *Mol. Syst. Biol.* **2** 0033

[7] Nelson D E, Ihekwaba A E C, Elliott M, Johnson J R, Gibney C A, Foreman B E, Nelson G, See V, Horton C A and Spiller D G *et al* 2004 Oscillations in NF-kB signaling control the dynamics of gene expression *Science* **306** 704–8

[8] Bosisio D, Marazzi I, Agresti A, Shimizu N, Bianchi M E and Natoli G 2006 A hyper-dynamic equilibrium between promoter-bound and nucleoplasmic dimers controls NF-kappaB-dependent gene activity *EMBO J.* **25** 798–810

[9] Metivier R, Penot G, Hubner M R, Reid G, Brand H, Kos M and Gannon F 2003 Estrogen receptor-alpha directs ordered, cyclical, and combinatorial recruitment of cofactors on a natural target promoter *Cell* **115** 751–63

[10] Kucho K, Okamoto K, Tsuchiya Y, Nomura S, Nango M, Kanehisa M and Ishiura M 2005 Global analysis of Circadian expression in the cyanobacterium Synechoscystis sp. Strain PCC 6803 *J. Bacteriol.* **187** 2190–9

[11] Berridge M J, Bootman M D and Roderick H L 2003 Calcium signalling: dynamics, homeostasis and remodelling *Nat. Rev. Mol. Cell Biol.* **4** 517–29

[12] Hirata H, Yoshiura S, Ohtsuka T, Bessho Y, Harada T, Yoshikawa K and Kageyama R 2002 Oscillatory expression of the bHLH factor Hes1 regulated by a negative feedback loop *Science* **298** 840–3
[13] Pourquié O 2003 The segmentation clock: converting embryonic time into spatial pattern *Science* **301** 328–30
[14] Aulehla A and Herrmann B G 2004 Segmentation in vertebrates: clock and gradient finally joined *Genes Dev.* **18** 2060–7
[15] Dequeant M L, Glynn E, Gaudenz K, Wahl M, Chen J, Mushegian A and Pourquié O 2006 A complex oscillating network of signaling genes underlies the mouse segmentation clock *Science* **314** 1595–8
[16] Haupt Y, Maya R, Kazaz A and Oren M 1997 Mdm2 promotes the rapid degradation of p53 *Nature* **387** 296–9
[17] Lahav G 2004 The strength of indecisiveness: oscillatory behavior for better cell fate determination *Science's STKE* **2004** pe55
[18] Chadwick D J and Goode J A (ed) 2003 *Mechanisms and Biological Significance of Pulsatile Hormone Secretion Series: Novartis Foundation Symp*. (New York: Wiley)
[19] Golden S S, Ishiura M, Johnson C H and Kondo T 1997 *Annu. Rev. Plant Physiol. Plant Mol. Biol.* **48** 327–54
[20] Krishna S, Andersson A M C, Semsey S and Sneppen K 2006 Structure and function of negative feedback loops at the interface of genetic and metabolic networks *Nucl. Acids Res.* **34** 2455–62
[21] Thomas R 1981 *Quantum Noise (Springer Series in Synergetics 9)* ed Gardiner (Berlin: Springer) pp 180–93
[22] Snoussi E H 1998 Necessary conditions for multistationarity and stable periodicity *J. Biol. Sys.* **6** 3–9
[23] Gouzé J L 1998 Positive and negative circuits in dynamical systems *J. Biol. Syst.* **6** 11–5
[24] Schnarr M *et al* 1991 DNA binding properties of the LexA repressor *Biochimie* **73** 423–31
[25] Wu X, Bayle J H, Olson D and Levine A J 1993 The p53-mdm-2 autoregulatory feedback loop *Genes Dev.* **7** 1126–32
[26] Dodd I B, Perkins A J, Tsemitsidis D and Egan J B 2001 Octamerization of lambda CI repressor is needed for effective repression of PRM and efficient switching from lysogeny *Genes Dev.* **15** 3013–22
[27] Semsey S, Virnik K and Adhya S 2006 Three-stage regulation of the Amphibolic gal operon: from repressosome to GalR-free DNA *J. Mol. Biol.* **358** 355–63
[28] Strogatz S 1994 *Nonlinear Dynamics and Chaos* (Reading, MA: Addison-Wesley)
[29] Mallet-Paret J and Smith H L 1990 The Poincare-Bendixson theorem for monotone cyclic feedback systems *J. Dyn. Diff. Eqns* **2** 367–421
[30] Tiana G, Jensen M H and Sneppen K 2002 Time delay as a key to apoptosis induction in the p53 network *Eur. Phys. J. B* **29** 135–9
[31] Press W H 1992 *Numerical Recipes in C* (Cambridge: Cambridge University Press)
[32] Jensen M H, Sneppen K and Tiana G 2003 Sustained oscillations and time delays in gene expression of protein Hes1 *FEBS Lett.* **541** 176–7
[33] Lewis J 2003 Autoinhibition with transcriptional delay: a simple mechanism for the zebrafish somitogenesis oscillator *Curr. Biol.* **13** 1398–408
[34] Elowitz M B and Leibler S 2000 A synthetic oscillatory network of transcriptional regulators *Nature* **403** 335–8
[35] Goodwin B C 1965 *Adv. Enzyme Regulation* Vol 3 ed G Weber (Oxford: Pergamon) pp 425–38
[36] Bliss R D, Painter P R and Marr A G 1982 Role of feedback inhibition in stabilizing the classical operon *J. Theor. Biol.* **97** 177–93
[37] Guantes R and Poyatos J F 2006 Dynamical principles of two-component genetic oscillators *PLoS Comput. Biol.* **2** e30
[38] Conrad E D 1999 Mathematical models of biochemical oscillation *Master's Thesis*
[39] Ribbeck K and Gorlich D 2001 Kinetic analysis of translocation through nuclear pore complexes *EMBO J.* **20** 1320–30
[40] Alberts B, Bray D, Lewis J, Raff M, Roberts K and Watson J *Molecular Biology of the Cell* (New York: Garland)
[41] Picksley S M and Lane D P 1993 The p53–Mdm2 autoregulatory feedback loop: a paradigm for the regulation of growth control by p53? *Bioessays* **15** 689–90
[42] Bar-Or R L, Maya R, Segel L A, Levine A J and Oren M 2000 Generation of oscillations by the p53–Mdm2 feedback loop: a theoretical and experimental study *Proc. Natl Acad. Sci. USA* **97** 11250–6
[43] Schon O, Friedler A, Bycroft M, Freund S M V and Fersht A R 2002 Molecular mechanism of the interaction between MDM2 and p53 *J. Mol. Biol.* **323** 491
[44] Gottlieb T and Oren M 1996 p53 in growth control and neoplasia *Biochim. Biophys. Acta* **1287** 77–102
[45] Greenblatt M S, Bennett W P, Hollstein M and Harris C C 1994 Mutations in the p53 tumor suppressor gene: clues to cancer etiology and molecular pathogenesis *Cancer Res.* **54** 4855–78
[46] Mihalas M, Neamtu M, Opris D and Horhat F R 2006 A dynamic P53-MDM2 model with time delay *Chaos Solitons Fractals* **30** 936–45
[47] Kageyama R, Ishibashi M, Takebayashi K and Tomita K 1997 bHLH transcription factors and mammalian neuronal differentiation *Int. J. Biochem. Cell Biol.* **29** 1389
[48] Basak S *et al* 2007 A fourth IkappaB protein within the NF-kappaB signaling module *Cell* **128** 369–81
[49] Pahl H L 1999 Activators and target genes of Rel/NF-kappaB transcription factors *Oncogene* **18** 6853–66
[50] Kearns J D, Basak S, Werner S L, Huang C S and Hoffmann A 2006 IkBe provides negative feedback to control NF-κB oscillations, signaling dynamics, and inflammatory gene expression *J. Cell Biol.* **173** 659–64
[51] Krishna S, Jensen M H and Sneppen K 2006 Minimal model of spiky oscillations in NF-κB signaling *Proc. Natl Acad. Sci. USA* **103** 10840–5
[52] Hayot F and Jayaprakash C 2005 NF-kB oscillations and cell-to-cell variability *J. Theor. Biol.* **240** 583–91
[53] Lipniacki T, Paszek P, Brasier A R, Luxon B and Kimmel M 2004 Mathematical model of NF-kB regulatory module *J. Theor. Biol.* **228** 195–215
[54] Huang C–Y and Ferrel J E Jr 1996 Ultrasensitivity in the mitogen-activated protein kinase cascade *Proc. Natl Acad. Sci. USA* **93** 10078–83
[55] Goldbeter A and Koshland D E 1981 An amplified sensitivity arising from covalent modification in biological systems *Proc. Natl Acad. Sci. USA* **78** 6840–4
[56] Pigolotti S, Krishna S and Jensen M H 2007 Oscillation patterns in negative feedback loops *Proc. Natl Acad. Sci. USA* **104** 6533–7
[57] Ishiura M, Kutsuna S, Aoki S, Iwasaki H, Andersson C R, Tanabe A, Golden S S, Johnson C H and Kondo T 1998 Expression of a gene cluster kaiABC as a circadian feedback process in cyanobacteria *Science* **281** 1519–23
[58] Goldbeter A 1991 A minimal Cascade model for the Mitotic oscillator involving cyclin and cdc2 kinase *Proc. Natl Acad. Sci. (USA)* **88** 9107–11
[59] Igoshin O A, Goldbeter A, Kaiser D and Oster G 2004 A biochemical oscillator explains several aspects of Myxococcus xanthus behavior during development *Proc. Natl Acad. Sci. USA* **101** 15760–5

[60] Jacquet H, Renault G, Lallet S, Mey J D and Goldbeter A 2003 Oscillatory nucleocytoplasmic shuttling of the general stress response transcriptional activators Msn2 and Msn4 in Saccharomyces cerevisiae *J. Cell Biol.* **161** 497–505

[61] Leloup J C and Goldbeter A 2003 Toward a detailed computational model for the mammalian circadian clock *Proc. Natl Acad. Sci. USA* **100** 7051–6

[62] Reidl J, Borowski P, Sensse A, Starke J, Zapotocky M and Eiswirth M 2005 Model of calcium oscillations due to negative feedback in olfactory cilia *Biophys. J.* **90** 1147–55

[63] Goldbeter A, Dupont G and Berridge M 1990 Minimal model for signal-induced Ca_{2+} oscillations and for their frequency encoding through protein phosphorylation *Proc. Natl Acad. Sci. USA* **87** 1461–5

[64] Barken D, Wang C J, Kearns J, Cheong R, Hoffmann A and Levchenko A 2005 Comment on 'Oscillations in NF-κB signaling control the dynamics of gene expression' *Science* **308** 52a

[65] Ting A Y and Endy D 2002 Decoding NF-κB signaling *Science* **298** 1189–90

[66] Glass L and McKey M C 1988 *From Clocks to Chaos* (Princeton, NJ: Princeton University Press)

[67] Hayes N D 1950 Roots of transcendental equations associated with certain difference-differential equations *J. Lond. Math. Soc.* **25** 226–32